

# Biocomposites Based on Sea Algae Fibers and Biodegradable Thermoplastic Matrices

S. IANNACE, G. NOCILLA, L. NICOLAIS

Institute of Composite Material Technology (ITMC-CNR) & Department of Materials and Production Engineering (DIMP), University of Naples "Federico II", P.le Tecchio 80, 80125 Naples, Italy

Received 13 July 1998; accepted 28 December 1998

**ABSTRACT:** Composites were prepared by mixing thermoplastic biodegradable polymers with sea algae fibers. Tensile mechanical properties were analyzed as a function of fiber concentration. The effect of processing, such as compression molding and calendering, on the mechanical properties of the materials was investigated. Composites showed higher elastic modulus and lower strength than the matrix components. Fiber damaging, characterized by a reduction of both length and diameter, was observed in the composites. Films, prepared by calendering operations, showed anisotropic properties due to fiber alignment. © 1999 John Wiley & Sons, Inc. *J Appl Polym Sci* 73: 583–592, 1999

**Key words:** biodegradable composites; natural fibers; mechanical properties; processing

## INTRODUCTION

Environmental concerns generated by plastic materials are generating an increasing interest toward the development of ecological products. The use of disposable plastic material increases the undegradable waste portion; and, for this reason, it is necessary to develop more recyclable and/or biodegradable plastic to reduce the amount of plastic to landfill.

Biodegradable polymers are already utilized in many biomedical applications, such as biodegradable sutures, wound dressing, bioresorbable implants, and drug delivery systems, applications where the high cost of the materials is justified. However, their use in commodity applications, such as packaging or agriculture, is still limited either for economical reasons and for difficulties related to their processing, often due to their poor thermal stability.

Among the most interested biodegradable polymers studied today, we should mention the microbial polyesters; the synthetic polyesters, such as polylactide, polyglycolide, and their copolymers; polycaprolactone; and biopolymers, such as starch and polysaccharides, obtained from renewable sources. The combination of these materials in blends and/or composites allows the preparation of polymeric systems whose properties can be tailored for specific applications. Blends and composites of starch with natural and/or synthetic polymers have been extensively studied, and this issue has been recently reviewed.<sup>1–3</sup> In our previous works, we have reported on the effect of the composition on the properties of partially and totally biodegradable blends, such as poly(methyl methacrylate) and polycaprolactone (PMMA-PCL) blends,<sup>3</sup> polyhydroxybutyrate-co-valerate, and poly-L-lactide (PHB-PLLA) blends<sup>4,5</sup> and on starch-based polyurethane foams.<sup>6</sup>

Properties and cost of biodegradable polymers can be modified and improved through the use of natural occurring fibers that reduce the cost of the material without modifying their biodegrad-

---

Correspondence to: S. Iannace.

*Journal of Applied Polymer Science*, Vol. 73, 583–592 (1999)

© 1999 John Wiley & Sons, Inc.

CCC 0021-8995/99/040583-10

ability. The advantage of using vegetal fibers is that they can be produced by a large amount of different kind of plants; therefore, they can be obtained by renewable sources distributed around the world. Lignocellulosic fibers have been used with not degradable polymers, such as polypropylene,<sup>7–11</sup> polyethylene,<sup>12–15</sup> polyvinyl chloride, and polystyrene<sup>16–18</sup> to reduce the cost of these commodity thermoplastics. Most of the prior works on lignocellulosic fibers in thermoplastics deal with the use of wood flour and native cellulose fibers, such as kenaf, jute, flax, and sisal, with additives that can improve dispersion and interaction with the polymeric matrix. The use of the lignocellulosic materials in these thermoplastics results in material with higher elastic modulus. Their strength is usually lower due to the poor adhesion between the hydrophilic filler and the hydrophobic matrix. As a matter of fact, fibers can work as reinforcement or as filler, depending on the fiber–matrix interaction, on the aspect ratio and on the critical fiber length. A strong interface is necessary to obtain stress transfer from the matrix to the fibers and to avoid that the dispersed phase acts like weak points in the material. Reinforcing effects can be improved, therefore, if the adhesion is promoted by the use of additives or by chemical modifications of the components.

One of the possibilities is to functionalize the polymeric matrix, for example, with maleic anhydride, to increase the hydrophilic characteristics of the polymer. Treatment of the fiber surface is another technique<sup>7,9,11,14–16,19,20</sup> that improves the compatibility between the surface energies of the two phases, but the addition of a processing step may increase the cost of the material. A recent review deals with advantages and drawbacks of the different approaches.<sup>21</sup>

In this work, biodegradable composites were prepared by using sea algae fibers, as lignocellulosic fibers, embedded in three different biodegradable polymeric matrices. Effects of processing and fiber composition on mechanical properties were investigated.

## EXPERIMENTAL

### Materials

The following three polymers were used as the matrix: Mater-Bi<sup>®</sup> YI01 U (MAT-Y) and Mater-Bi<sup>®</sup> ZF03 U/A (MAT-Z) (kindly supplied by Nova-

mont, Italy) and polycaprolactone (PCL) (Aldrich Chemical Company, USA;  $M_n = 42,500$ ).

The fibers utilized in this work were algae collected from Sardinia (Italy) beaches. They were first used for agricultural applications in hydroponic cultures in greenhouses for 2 years. They were dried at 40°C in a vacuum oven for 24 h prior the preparation of the composites.

### Processing

Composites were prepared with the following different processing technologies: batch compounding, extrusion, compression molding, and calendaring.

Fibers were dispersed in the polymers in a mix chamber (Rheocord 9000 HAAKE) at different fiber concentrations. Compounds were compression-molded, and these materials will be referred as MIX-COMP. Compounding, before compression-molding, was also performed by using a laboratory twin-screw extruder (HAAKE CTW 100) to prepare pellets. These pellets were then either compression-molded (samples EXT-COMP) or used to prepare films by a calendaring device (samples EXT-CAL).

### MIX-COMP

The following fiber concentrations were used in this case: MAT-Y, 5–50% *w* with increments of 5% *w*; MAT-Z, 5–40% *w*, with increments of 5% *w*; and PCL, 30–70% *w* with increments of 10% *w*.

Mixing temperatures were 72°C for MAT-Z and 140°C for MAT-Y, and they were chosen according to the technical specifications indicated for the different grades of Mater-Bi. PCL-based composites were processed at 140°C because, at this temperature, the low viscosity of the matrix allowed the preparation of samples with high fiber concentration. The rotational speed was kept equal to 100 rpm, and the residence time varied from 60 to 150 s with the increase of the fiber content.

Compression-molding was performed with a pressure of 0.7 MPa and a temperature of 180°C for MAT-Y-based composites and 0.35 MPa and 90°C for both MAT-Z- and PCL-based materials.

### EXT-COMP

Compounding was performed by the twin-screw extruder to prepare pellets having a fiber concentration of 40% *w* in a matrix of MAT-Z. Due to the low density of the lignocellulosic materials, the

fiber dispersion in the extruder was divided in four steps: the material was extruded four times; and, at each step, fibers were added with increments of 10% in order to get an overall fiber content of 40% *w*. The total residence time of the polymer in the extruder after the four stages was kept equal to 180 s, that is, 30 s more than the mixing time in the Rheocord. The temperature in the extruder can be independently controlled in four zones: three along the barrel, and the last at the die. In this case, the four temperatures were 50, 75, and 90°C in the barrel and 110°C at the die. Compression-molding was performed according to the procedures described above.

### EXT-CAL

Composite pellets with MAT-Z were prepared with a fiber content of 30% *w* and then calendered. Also in this case, the extrusion process was divided into three steps to increase progressively the fiber content and the temperature profile was the same as in the previous section. A fourth step, with the same temperature profile, was then employed for the calendering operation.

### Test Methods

Tensile tests were performed by an INSTRON (model 4204) according to the ASTM 638M (dumb-bell geometry Type M-III). Crosshead speed employed for the tests was 2 mm/min. Morphology of the fracture surfaces was observed by means of a scanning electron microscopy (HITACHI S-2300).

### Statistical Distribution of Fiber Geometry

Fiber length and diameter were statistically evaluated on the composite samples after removal of the matrix component by Soxhlet extraction. Experimental data were elaborated in order to obtain the cumulative distribution function of fiber dimensions:  $F(d)$  for diameter,  $F(l)$  for length, and  $F(l/d)$  for the aspect ratio. In general, the function  $F(x)$  describes the fraction of fibers having a dimension  $\leq x$ .

## RESULTS AND DISCUSSION

### Mechanical Properties

Biodegradable polymers with different mechanical properties were selected as matrices. MAT-Y is a brittle polymer with a high modulus ( $E = 793$

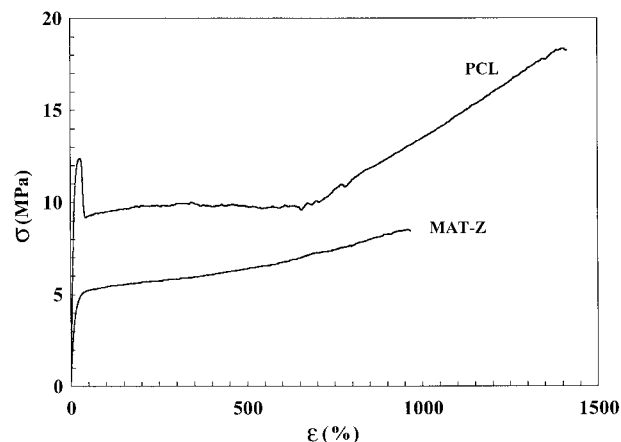


**Figure 1** Stress–strain curves of MAT-Z and PCL.

MPa) and low elongation at break ( $\epsilon_b = 4.9\%$ ), while MAT-Z ( $E = 38$  MPa) and PCL ( $E = 114$  MPa) are flexible materials with very high  $\epsilon_b$  ( $\epsilon_b$  equal to 1480% for PCL and 960% for MAT-Z). In particular, PCL displays the typical cold drawing behavior with the formation of a neck, which appears in correspondence to the yielding stress (Fig. 1). The formation of the neck is followed by a plastic flow occurring with almost constant stress up to a deformation of 700%. The alignment of the macromolecules, which follows this phenomena, produces a further increase of the stress versus strain up to rupture of the material. MAT-Z shows a very high elongation at break; but, in this case, no neck was observed, and, for this reason, the yield point does not exhibit the typical maximum, as shown in the same figure.

Selected stress–strain curves are reported in Figures 2–4 to show the effect of fibers concentration on the mechanical behavior of the composites, while Tables I–III report mechanical data of the all materials prepared. The three classes of materials present a similar behavior: an increase of the amount of fibers results in higher elastic modulus and lower strength and maximum elongation, compared to the properties of the matrix components.

Fibers produce a great reduction of the maximum elongation displayed by the pure MAT-Z and PCL. In MAT-Z-based composites, fibers progressively reduce the plastic flow (Fig. 3), which disappears at a concentration above 20%.

Cold drawing is absent in PCL-based composites (Fig. 4), and this is due to the high concentration of fibers (>30%). In this case, a yield point is still present, but the presence of fibers prevents macromolecular orientations, typical of the cold-

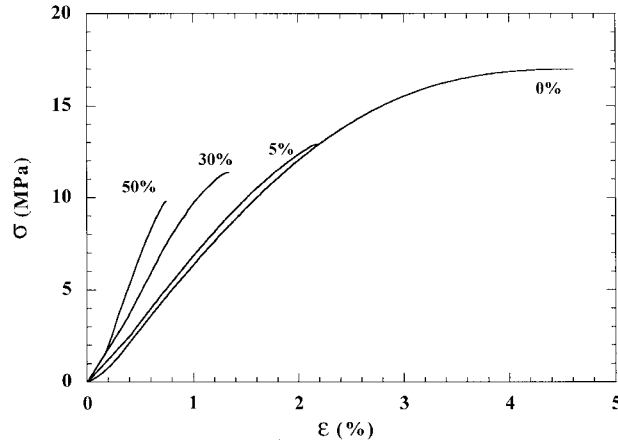


**Figure 2** Stress-strain curves of the MAT-Y composites.

drawing phenomena. However, composites with fiber concentration up to 50% do not display brittle fracture. As a matter of fact, postyielding behavior is characterized by a gradual reduction of the stress upon strain, and this can be correlated to fiber pull-out.

Comparison among three composite materials reinforced with the same fiber concentration (30% *w*) is shown in Figure 5. Differences of the mechanical behavior of the pure polymers are strongly reduced in the composites. As a matter of fact, elongation at break varies only from 1.3 to 3.5%, strength from 5.5 to 11 MPa, and the modulus from 363 to 1166 MPa. Contribution of the fiber properties to the mechanical behavior of the composite becomes more and more significant as the fiber concentration increases.

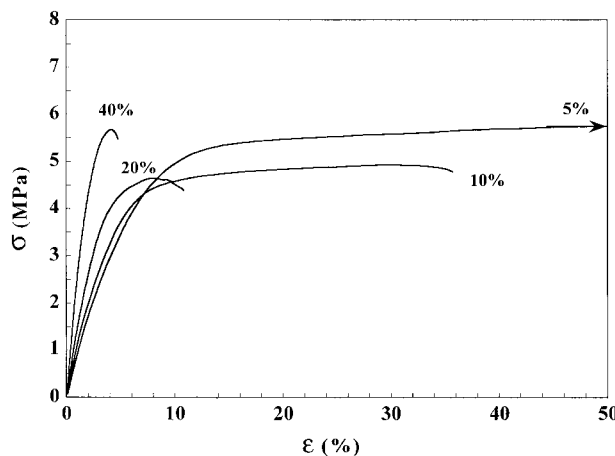


**Figure 3** Stress-strain curves of the MAT-Z composites.

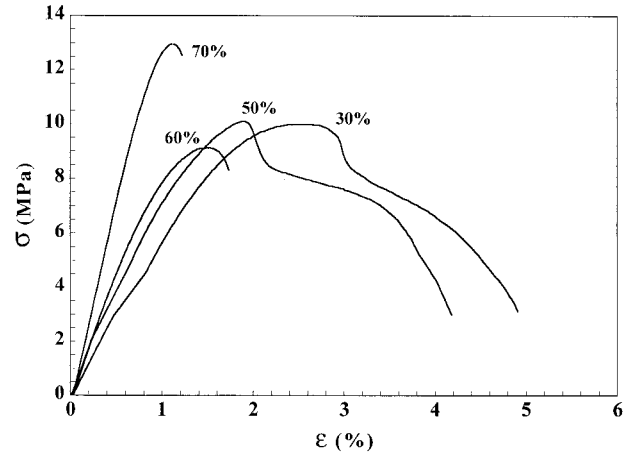


**Figure 4** Stress-strain curves of the PCL composites.

### Elastic Modulus

The higher elastic modulus of the fibers, compared to those of the matrices employed in this work, lead to materials with greater rigidity. In order to examine this behavior, experimental data were analyzed according to the Halpin-Tsai equation, as follows:

$$\frac{E_c}{E_m} = \frac{(1 + AB\phi)}{(1 - B\phi)} \quad (1)$$

with

$$B = \frac{E_f/E_m - 1}{E_f/E_m + A} \quad (2)$$

**Table I** Mechanical Data of MAT-Y-Based Composites (MIX-COMP)

Algae Content (%)	$E$ (MPa)	$\sigma_b$ (MPa)	$\varepsilon_b$ (%)
0 <i>w</i>	792.8 ± 14.3	17.0 ± 1.0	4.9 ± 0.2
5 <i>w</i>	827.7 ± 46.3	12.5 ± 0.3	2.2 ± 0.1
10 <i>w</i>	1050.1 ± 49.6	11.0 ± 1.7	1.5 ± 0.2
15 <i>w</i>	744.9 ± 141.9	5.6 ± 1.1	0.8 ± 0.1
20 <i>w</i>	898.0 ± 221.9	6.8 ± 1.3	1.0 ± 0.1
25 <i>w</i>	1155.6 ± 266.8	10.7 ± 1.5	1.1 ± 0.2
30 <i>w</i>	1166.1 ± 88.1	9.6 ± 1.5	1.0 ± 0.2
35 <i>w</i>	1139.8 ± 172.2	10.1 ± 1.5	0.9 ± 0.1
40 <i>w</i>	1253.4 ± 638.9	10.8 ± 1.0	0.8 ± 0.1
45 <i>w</i>	1825.7 ± 327.6	10.5 ± 2.4	0.8 ± 0.1
50 <i>w</i>	2207.9 ± 403.7	9.9 ± 1.1	0.7 ± 0.1

**Table II Mechanical Data of MAT-Z-Based Composites (MIX-COMP)**

Technology	Algae Content (%)	$E$ (MPa)	$\sigma_y$ (MPa)	$\varepsilon_y$ (%)	$\sigma_b$ (MPa)	$\varepsilon_b$ (%)
MIX-COMP	0 w	37.5 ± 0.9	2.4 ± 0.6	6.6 ± 1.5	7.3 ± 1.3	859.0 ± 89.0
MIX-COMP	5 w	76.4 ± 4.8	3.3 ± 0.4	4.5 ± 0.7	5.5 ± 0.3	106.3 ± 16.5
MIX-COMP	10 w	89.5 ± 12.1	1.8 ± 0.3	2.5 ± 0.5	4.3 ± 0.7	53.5 ± 24.7
MIX-COMP	15 w	138.0 ± 9.3	2.5 ± 0.3	2.0 ± 0.3	5.0 ± 0.1	18.6 ± 6.1
MIX-COMP	20 w	181.8 ± 21.8	2.0 ± 0.1	1.3 ± 0.1	4.7 ± 0.6	14.3 ± 3.9
MIX-COMP	25 w	226.5 ± 70.7	2.6 ± 0.4	1.4 ± 0.5	4.6 ± 0.1	3.7 ± 1.3
MIX-COMP	30 w	363.2 ± 29.7	2.6 ± 0.3	0.9 ± 0.1	5.5 ± 0.8	3.2 ± 0.2
EXT-CAL	30 w	590.6 ± 41.8	7.5 ± 0.8	1.5 ± 0.1	8.8 ± 0.9	2.5 ± 0.2
MIX-COMP	40 w	333.5 ± 10.3	3.0 ± 0.2	1.1 ± 0.2	5.6 ± 0.5	4.0 ± .04
EXT-COMP	40 w	233.8 ± 7.5	2.6 ± 0.1	1.3 ± 0.3	7.2 ± 0.6	9.1 ± 0.7

where  $E_c$ ,  $E_m$ , and  $E_f$  are the elastic modulus of the composite, the matrix, and the fibers;  $\phi$  is the volumetric fiber concentration. The elastic modulus of the fibers was assumed to be equal to 5.62 GPa (see discussion on morphology for details).

$A$  is a not negative parameter related to (a) fiber aspect ratio  $l/d$ , (b) packing geometry, and (c) loading conditions.  $A$  was used as an adjustable parameter for the fitting of the experimental data, and the following values were found:  $A = 0.615$  for MAT-Y,  $A = 14.9$  for MAT-Z,  $A = 6.09$  for PCL. A comparison between experimental data and the best fitting curves obtained by eqs. (1)–(2) is reported in Figure 6.

The low value of  $A$  and, therefore, the small increase of the elastic modulus observed in the composite with MAT-Y is due to damaging effects occurring during the mixing process of the fibers in the melt, as confirmed by lower values of the statistical distribution of the aspect ratio reported in Figure 7(a). Less damage was observed when MAT-Z and PCL were used as matrices, and this is related to their lower viscosity during the mixing process. As a matter of fact, high shear stresses developed during mixing can result in

the breakage of the fibers if the shear stresses transferred to the fibers overcome their tensile strength, and this effect was more evident in MAT-Y-based composites.

Shear stresses result not only in the fragmentation of the fibers but, as confirmed by the statistical analysis of fiber diameter [Fig. 7(b)], induce their disgregation into fibers constituted by a discrete number of individual fibers or ducts, promoting an effective reduction of the average diameter of the reinforcing elements. The distribution function  $F(d)$  is not continuous with the diameter but has a typical multimodal shape. This is due to the fact that disgregation leads to fibers composed by an integer number of elementary fibrils.

These individual fibers are themselves composites of predominantly cellulose, lignin, and hemicellulose; and their mechanical properties are dependent on the cellulose content and also on the angle at which fibrils are aligned in the fibers. Finally, the mechanical properties of the overall fiber is dependent on the properties of the matrix connecting the individual fibers, which usually is the weak link in the system.

**Table III Mechanical Data PCL-Based Composites (MIX-COMP)**

Algae Content (%)	$E$ (MPa)	$\sigma_y$ (MPa)	$\varepsilon_y$ (%)	$\sigma_b$ (MPa)	$\varepsilon_b$ (%)
0 w	114.1 ± 1.1	7.2 ± 0.3	6.5 ± 0.1	18.2 ± 0.5	1426.4 ± 8.2
30 w	557.8 ± 132.7	7.2 ± 0.7	1.7 ± 0.7	9.8 ± 0.6	3.3 ± 1.2
40 w	630.2 ± 28.4	8.4 ± 1.0	1.5 ± 0.1	9.7 ± 0.5	2.2 ± 0.3
50 w	847.5 ± 120.8	6.8 ± 1.9	1.0 ± 0.2	9.2 ± 1.3	1.8 ± 0.3
60 w	1170.7 ± 18.8	7.0 ± 1.9	0.8 ± 0.1	9.1 ± 1.3	1.4 ± 0.2
70 w	1468.6 ± 32.3	12.1 ± 0.9	1.0 ± 0.1	12.7 ± 1.2	1.2 ± 0.1

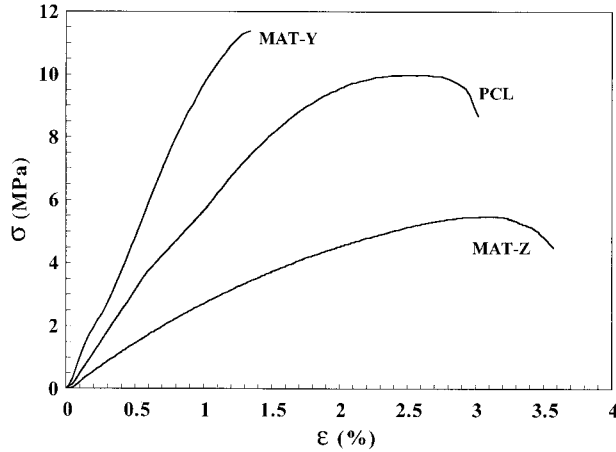


**Figure 5** Effect of the matrix on the stress–strain curves of composites containing 30% *w* of fibers.

Comparison between the statistical distribution of the fiber diameter in PCL and MAT-Z composites, reported in Figure 7(b), shows that the disgregation of the original fibers is less pronounced in PCL-based composites. Here, a relatively high percentage of fibers (~ 30%) have a greater diameter than those dispersed in MAT-Z-based composites. As a consequence, in the PCL systems, load is carried by a high number of fibers composed of a certain number of adjacent ducts; and, for this reason, the effect on Young’s modulus of the composites is less effective than in systems, where the individual fibers are separated. This behavior justifies the lower value of *A* in PCL composites compared to the MAT-Z-based composites.

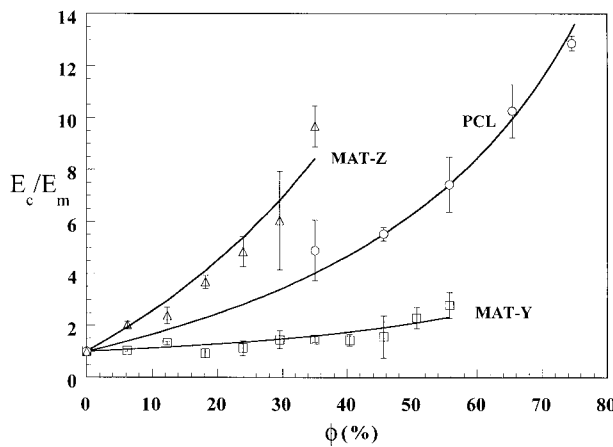


**Figure 6** Normalized elastic modulus of the composites as function of fiber concentration. Continuous curves represent the Halpin–Tsai model.

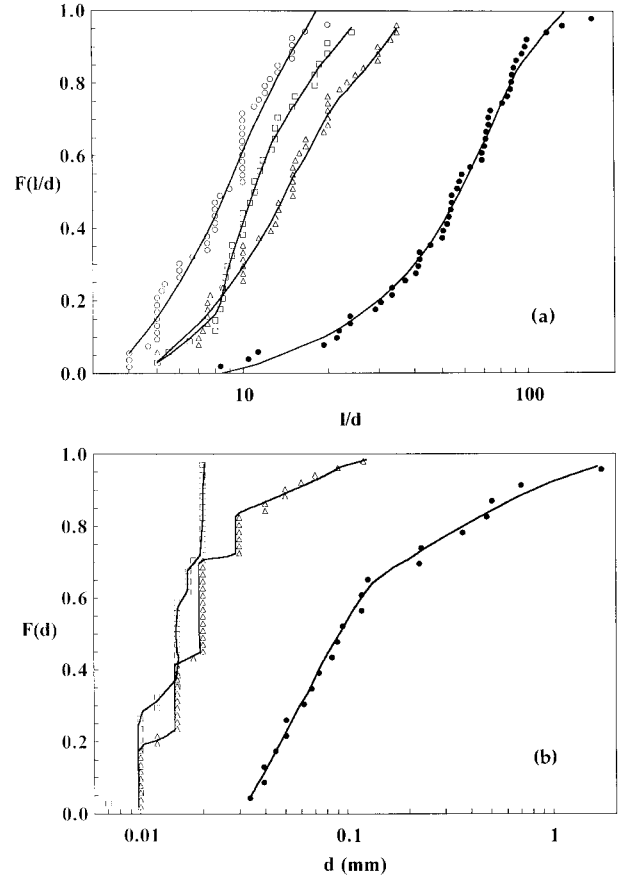


**Figure 7** Cumulative distribution of (a) aspect ratio  $l/d$  and (b) fiber diameter of MIX–COMP samples containing 30% *w* of fibers; (□), MAT-Z, (○) MAT-Y, (△) PCL, (●) fibers before processing.

### Mechanical Strength of Composites

The addition of fibers to the biodegradable matrices results in materials with lower mechanical strength. Strength of composites  $\sigma_{bc}$ , divided by the strength of the matrix  $\sigma_{bm}$  is reported in Figure 8 as function of fiber concentration. After an initial drop, there is an increase of  $\sigma_{bc}$  with a partial recovery of the mechanical strength.

In order to make comparison between the different composites, we should take into account the differences exhibited by the matrix components. The biodegradable polymers chosen for this work have very different mechanical behaviors, ranging from systems presenting high rigidity and brittle fracture (MAT-Y) to materials with plastic flow associated with cold drawing (PCL) and to materials displaying viscous flow (MAT-Z). For the last two composite systems, fracture occurs after the yielding point. In particular, for

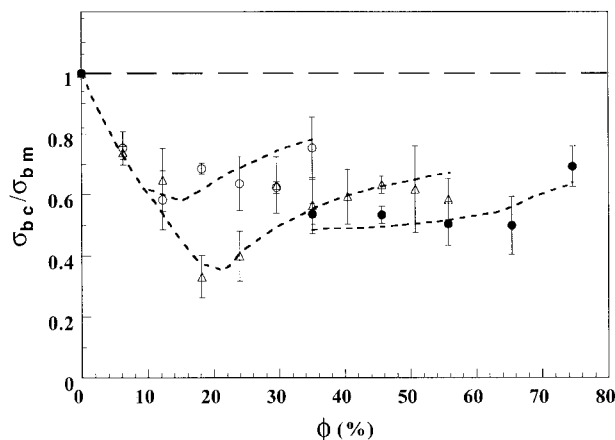


**Figure 8** Normalized mechanical strength versus fiber concentration: (○) MAT-Z, (△) MAT-Y, and (●) PCL.

MAT-Z-based composites, this is true when composition is lower than 15%  $w$ . In this case, fibers interfere with the alignment of the macromolecules during the plastic flow, amplifying defects and reducing the maximum strength of the material. For concentration higher than a critical value, plastic flow is not present, and the rupture occurs when the stress overcomes the strength of the composite system, which depends upon the reinforcing capacity of the fibers and the quality of the adhesion.

The initial decrease of the mechanical strength is, however, a common behavior in short fiber-reinforced composites<sup>22</sup> since a low volumetric fraction of fibers ( $\phi$ ) does not provide additional strength to the matrix. In other terms, at low concentrations, fibers act only like weakening points. When algae concentration is higher ( $>15\% w$  for MAT-Z;  $>25\% w$  for MAT-Y), fibers contribute to increase the strength of the material, allowing a partial recovery of the initial drop.

Comparison between MAT-Y and MAT-Z data confirms that damage of fibers is less pronounced in the latter system, probably for the low viscosity of the matrix and for the lower mixing temperature. We should underline that for fiber concentration higher than the minimum volumetric fraction allowable for reinforcing effects, mechanical strength doesn't increase monotonically with fiber concentration. As a matter of fact, the mechanical strength of the composites is never higher than the matrix strength, but, in the best case, it is about 40% lower. This is due to the poor mechanical strength of the algae fibers, which can be related to the low actual section of the porous

morphology displayed by these fibers, as will be discussed later. Moreover, the average length of the fibers is probably lower than the critical length necessary for reinforcing effects.

The higher strength displayed by MAT-Z composites, compared to PCL ones, can be related not only to a different level of fiber–matrix interaction of the two composite materials, but also to the greater fiber disgregation occurring in MAT-Z composites. In the latter case, load is transferred to fibers with a fewer numbers of ducts and, similarly, to what is observed for the elastic modulus, this produced materials with higher strength.

### Effect of Processing

In order to analyze the effect of the mixing process on the mechanical properties, composites based on MAT-Z, containing 40%  $w$ , of fibers were prepared according to procedures described above for MIX-COMP and EXT-COMP. Stress–strain curves, compared in Figure 9, show that extrusion process yields to materials with higher strength and strain at break (Table II).

The lower strength displayed by the MIX-COMP samples is related to the different damaging effects occurring during mixing and extrusion. The higher shear stresses, developed during the extrusion process, result in greater damaging of fibers, which showed a lower length [Fig. 10(a)] and diameter [Fig. 10(b)]. However, fragmentation and disgregation produce fibers with a higher aspect ratio  $l/d$  [Fig. 10(c)]. Combination of these two effects (separation in individual fibers and

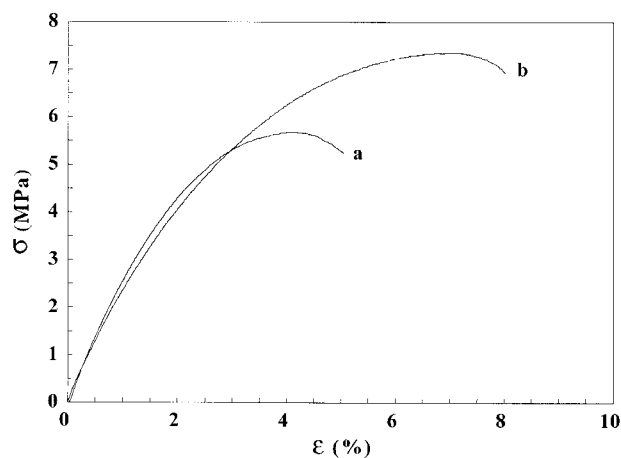


**Figure 9** Effect of processing on stress–strain curves of the MAT-Z-based composite, with a fiber concentration of 40%  $w$ : [curve (a)] MIX-COMP and [curve (b)] EXT-COMP.

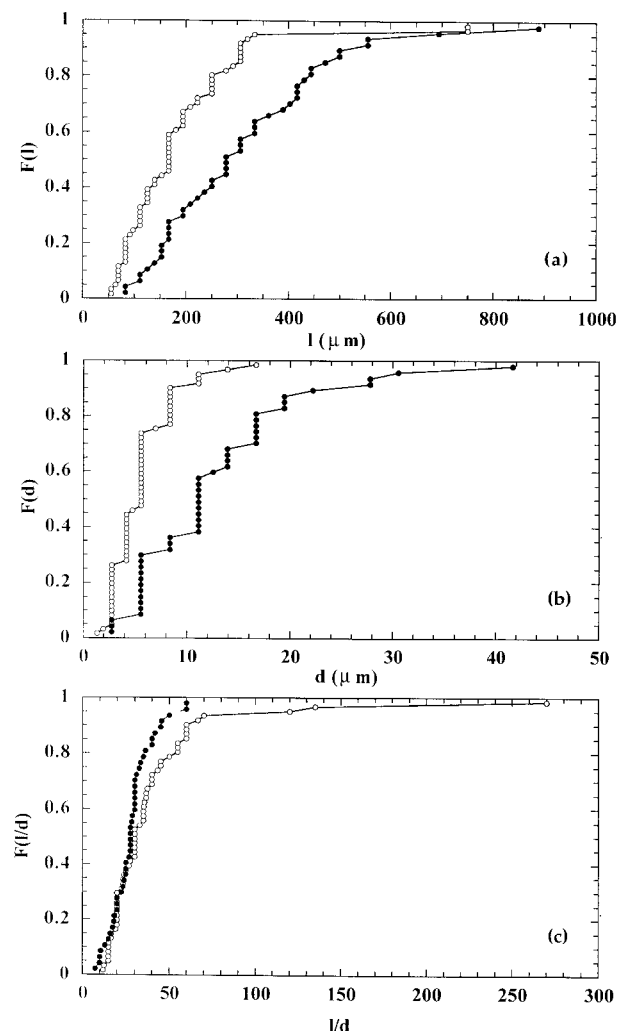


**Figure 10** Effect of processing on the cumulative distribution of (a) length, (b) fiber diameter, and (c) aspect ratio  $l/d$  on MAT-Z composites containing 40%  $w$  of fibers: (○) EXT-COMP and (●) MIX-COMP.

increase of  $l/d$ ) leads to composite materials with higher strength.

In Figure 11, stress–strain curves of MIX-COMP (30%  $w$  of fibers) samples [curve (a)] are compared with EXT-CAL (30%  $w$  of fibers) samples in the transversal [curve (b)] and longitudinal [curve (c)] directions of the calendering operation; also in this case, materials prepared by mixing show lower mechanical properties. Moreover, flow profiles developed during the calendering operation gave rise to anisotropic materials. For this reason, mechanical properties measured in the longitudinal direction are higher than those measured in the opposite one. This behavior is related to alignment of both fibers and poly-

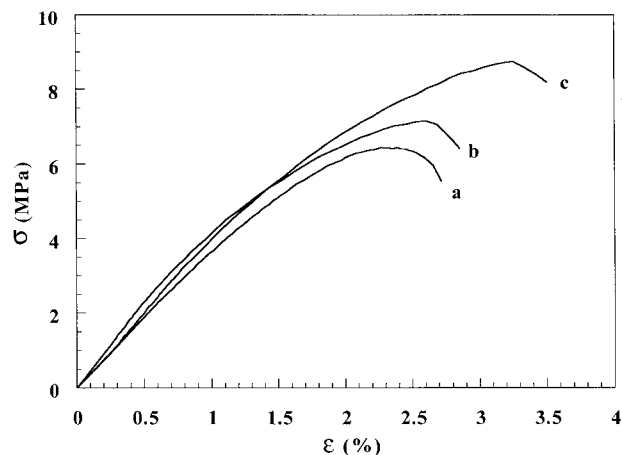


**Figure 11** Effect of processing on stress–strain curves of MAT-Z-based composite, with a fiber concentration of 30%  $w$ : [curve (a)] MIX-COMP, and [curve (b)] EXT-CAL in transversal and [curve (c)] longitudinal directions.

meric matrix. As a matter of fact, these directional effects were also observed in pure calendered MAT-Z.

### Morphology

Scanning electron microscopy of the algae revealed the cellular structure of these fibers (Fig. 12), characterized by a large number of adjacent ducts. The resistant section is therefore lower, and this is one of the reasons of the low mechanical strength of both fibers and composites. Image analysis of the algae section allowed the determi-

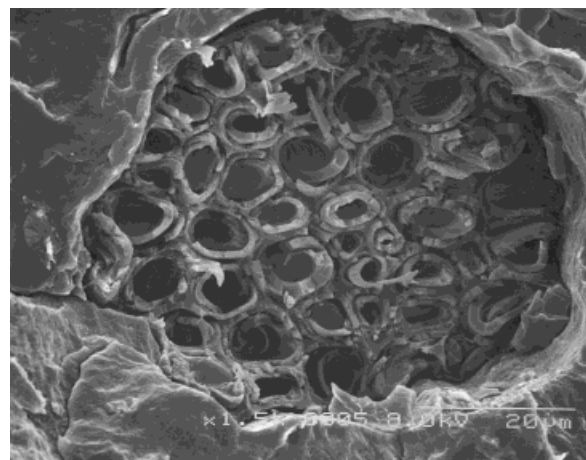
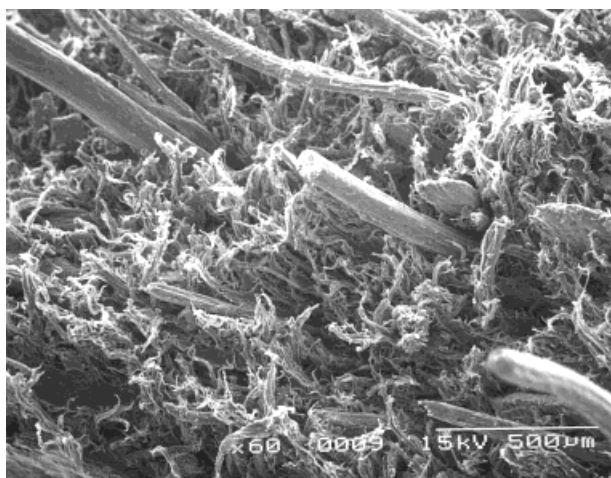
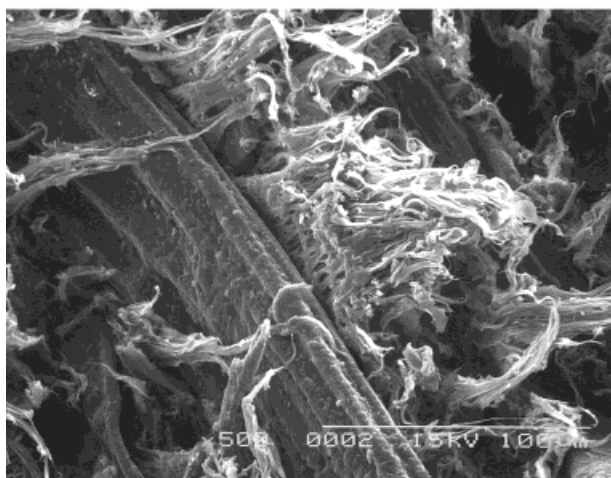


**Figure 12** Scanning electron microscopy (SEM) micrograph of the fracture section of an algae fiber (1500 $\times$ ).



(a)



(b)

**Figure 13** SEM micrograph of the fracture surface of the MAT-Z-based composites with 40% *w* of fibers: (a) 60 $\times$  and (b) 500 $\times$ .

nation of the void fraction ( $\sim 47\%$ ), which was used to estimate the properties of the fibers. Density and elastic modulus were calculated from the properties of crystalline cellulose, and the following values were obtained:  $\rho_{\text{fiber}} = 0.53 \cdot 1.50 \text{ g/cm}^3 = 0.795 \text{ g/cm}^3$ ; and  $E_{\text{fiber}} = 0.53 \cdot 10.6 \text{ GPa} = 5.62 \text{ GPa}$ .

Figure 13(a) shows the typical fracture surfaces of the MAT-Z-based composites. Even though fiber concentration in this figure is 40% *w* ( $\phi = 45.6\%$ ), the fiber fraction appears to be quite low. This is due to the damaging of the fibers that separate into a large number of small fibrils. As previously shown (Fig. 7), the initial size of the fibers is therefore reduced due to the separation of

the original adjacent ducts. These fibrils are embedded into the polymeric matrix and produce the typical fibrillar morphology when samples are mechanically loaded, as confirmed by the higher magnification micrograph [Fig. 13(b)]. Moreover, the surface of the fibers are not totally clean, and this suggested good fiber–matrix adhesion.

## CONCLUSIONS

The effect of sea algae concentration on the mechanical properties of biodegradable composites have been investigated. The increase of fiber content yields to materials with higher elastic modulus. However, due to the low mechanical strength of the fibers and to their low adhesion with the matrix, composites showed lower mechanical strength than those of the matrix constituents.

Shear stresses developed in mixing and extrusion processes were responsible for damaging phenomena of the fibers, and these effects are related to the different rheological properties of the thermoplastic matrices. Better mechanical properties were obtained in all those cases when a reduction of diameter, related to disaggregation of fibers, occurred, while the aspect ratio  $l/d$  was preserved.

The higher shear stresses developed in a counterrotating, conical, and intermeshing twin-screw extruder utilized to disperse fibers caused a great reduction of both fiber diameter and length. The statistical distribution of ratio  $l/d$  was, however, higher compared to those obtained from batch-mixing operations. For this reason, better mechanical properties were obtained when composites were prepared by the twin-screw extrusion process.

## REFERENCES

1. Bastioli, C. in *Degradable Polymers—Principles & Applications*, Scott, G.; Gilead, D., Eds.; Chapman & Hall: New York, 1995; chap. 6, pp. 112.
2. Bastioli, C.; Bellotti, V.; Camia, M.; Del Giudice, L.; Rallis, A. in *Biodegradable Polymers and Plastics*, Doi, Y.; Fukuda, K., Eds., Elsevier Science: New York, 1994; pp. 200–213.
3. Aminabhavi, T. M.; Balundgi, R. H.; Cassidy, P. E. in *Polymer–Plastic Technology*, Vol 29; 1990; pp. 235–262.

4. Iannace, S.; DeLuca, N.; Nicolais, L.; Carfagna, C. *J Appl Polym Sci* 1990, 41, 2691.
5. Iannace, S.; Ambrosio, L.; Huang, S. J.; Nicolais, L. *J Appl Polym Sci* 1994, 54, 1525.
6. Iannace, S.; Ambrosio, L.; Huang, S. J.; Nicolais, L. *J Macromol Sci Pure Appl Chem* 1995, A32, 881.
7. Raj, R. G.; Kotka, B. V.; Dembele, F.; Sanschagrain, B. *J Appl Polym Sci* 1989, 38, 1987.
8. Takase, S.; Shiraishi, N. *J Appl Polym Sci* 1989, 37, 645.
9. Felix, J. M.; Gatenholm, P. *J Appl Polym Sci* 1991, 42, 609.
10. Park, B.; Balatinecz, J. J. *Polym Compos* 1997, 18, 79.
11. Gassan, J.; Bledzki, A. K. *Composites Part A*, 1997, 28A, 1001.
12. Padilla Ramirez, A.; Sanchez Solis, A. *J Appl Polym Sci* 1984, 29, 2405.
13. Yam, K. L.; Gogol, B. K.; Lai, C. C.; Selke, S. E. *Polym Eng Sci* 1990, 30, 693.
14. Raj, R. G.; Kotka, B. V. *Polym Eng Sci* 1991, 31, 1358.
15. Raj, R. G.; Kotka, B. V.; Maldas, D.; Daneault, C. *J Appl Polym Sci* 1989, 37, 1087.
16. Maldas, D.; Kotka, B. V.; Deneault, C. *J Appl Polym Sci* 1989, 37, 751.
17. Czarnecki, L.; White, J. L. *J Appl Polym Sci* 1980, 25, 1217.
18. Maldas, D.; Kotka, B. V. *Polym Plast Technol Eng* 1990, 29, 119.
19. Bledzki, A. K.; Reihmane, S.; Gassan, J. *J Appl Polym Sci* 1996, 59, 1329.
20. Westerlind, B. S.; Berg, J. C. *J Appl Polym Sci* 1988, 36, 523.
21. Sanadi, A. R.; Rowell, R. M.; Caulfield, D. F. *Polym News* 1996, 20, 7.
23. Mallick, P. K. *Fiber-Reinforced Composites*, Marcel Dekker: New York, 1993.